engineering proceedings

MDPI

Proceedings Paper

Optimizing Cs2TiBr6-Based PSCs with Graphene Quantum Dots †

Riya Sen [1,2] *, Menka Yadav [1]

[1] Department of Electronics & Communication Engineering, Malaviya National Institute of Technical Studies, Jaipur, 302017, india; 2019rec9508@mnit.ac.in, menka.ece@mnit.ac.in
[2] Department of Electronics and Communications Engineering, Geetanjali Institute of Technical Studies, Udaipur, india;
* Correspondence: 2019rec9508@mnit.ac.in;
† Presented at the The 4th International Electronic Conference on Applied Sciences, 27 Oct–10 Nov 2023; Available online: https://asec2023.sciforum.net/

Abstract: The overall efficiency and optimization of the solar cell are significantly influenced by the selective layer in perovskite solar cells. In this study, particular emphasis is placed on the perovskite solar cell architecture, where both the charge transport layer is removed from the structure intentionally. In the paper, the full fabrication procedure is given free from the charge transport layer. To understand the behaviour of perovskite material, XRD analysis, TEM analysis along with photoluminescence measurements are conducted. These measurements provide valuable insights into the efficiency of the perovskite material. Additionally, SEM analysis is employed to characterize surface morphology of proposed structure. Furthermore, the photovoltaic performance of the proposed solar cell architectures is evaluated. With the addition of graphene quantum dots in perovskite solar cell's structure, we achieved an impressive 1.02% efficiency. The results show that, with a simple manufacturing procedure, removing the charge transport layer has the greatest influence on the photovoltaic performance. Overall, this research is helpful in understanding how cesium titanium bromide functions as an absorber in perovskite solar cells.

Keywords: Solar Cell; Cesium; Perovskite; Charge transport layer free;

Citation: To be added by editorial staff during production.

Academic Editor: Firstname Lastname

Published: date

1. Introduction

Perovskite solar cells (PSCs) excel in photovoltaics industries, boasting high power conversion efficiency (PCE) and cost-effective manufacturing. Their impressive PCE competes with advanced solar technology, promising greener energy. With low-cost, scalable production, PSCs redefine solar energy's landscape, driving sustainability and affordability in solar power. This remarkable progress has positioned PSCs as formidable competitors to other exciting solar cell technologies [1-3]. The unique properties of perovskite materials, such as broad absorption, a long diffusion length, and solution processability, make them exceptionally suitable as efficient light harvesters in PSCs [4-6]. PSCs can be categorized into three main architectures: Planar, Mesoporous, Inverted Structure. An additional potential function of some solar cells is the elimination of the HTL or the ETL, or even both. In such cases, the perovskite layer must perform the dual role of being a light harvester and a hole or electron conductor. The limited exploration of this simplest PSC configuration without ETL & HTL may stem from the complications faced by this device structure, particularly in terms of perovskite film deposition and charge extraction [7]. Addressing these issues, Tang et al. successfully designed a simplest PSC (FTO/$CsPbBr_3$/carbon) wherein $CsPbBr_3$ served as the light-absorbing material. Modifying FTO/$CsPbBr_3$ specially with $CsPbBrI_2$ quantum dots, and using porous FTO and NiO incorporated $MAPbI_3$ in the simplest PSC, boosted PCE to 4.1% [8]. Xiong et al. optimized

a basic MAPbI3 based PSC by introducing porous FTO and NiO within the perovskite layer [9]. Developing HTL or ETL free PSCs presents specific challenges. The absence of dedicated ETL or HTL leads to a heightened energy level difference between the perovskite layer and the metal contact or FTO glass, potentially causing recombination issues. Inherent electronic properties of materials must be optimized to compensate for the missing layers and ensure efficient charge carrier extraction. Additionally, careful solvent engineering is crucial to prevent solvent-related harm to underlying layers. These considerations are essential for achieving a stable and high-performance ETL- or HTL-free Perovskite Solar Cell.

In this study, we initially introduced and explored a ETL and HTL free PSC device structure consisting of FTO/Cs_2TiBr_6/Silver, achieving a PCE of 0.89%. Subsequently, by incorporating graphene quantum dots (GQDs) into the FTO/Cs_2TiBr_6/Ag structure, we enhanced the PCE to 1.02% under simulated AM1.5G solar illumination. Furthermore, we have delved into the characteristics of Cs_2TiBr_6 (a lead-free perovskite material) and examined its potential as a visible-light absorber for photovoltaic applications. The structure of the paper is as follows: Section 2 comprehensively covers the design and fabrication process of the PSC. Section 3 details the outcomes of our investigation, and lastly, Section 4 provides the concluding remarks of the paper.

2. Fabrication & Design of proposed PSC structure:

2.1. Synthesis of Cs_2TiBr_6 and PSC structure (FTO/Cs_2TiBr_6/Silver)

To synthesize Cs_2TiBr_6, a solution with di-isopropoxide bis(acetylacetonate) (TDBA; 50 µl, 0.10 mmol), Cs_2CO_3 (35 mg, 0.10 mmol), Oleylamine (OlAm; 0.60 ml), and Oleic Acid (OA; 1.0 ml) was mixed. After two hours of vacuum-assisted reflux in a 25 mL round-bottom flask for dryness, magnetic stirring at 330 RPM removed impurities, aiding Cs_2TiBr_6 nanocrystal synthesis. Following precursor preparation, quick TMS-Br (0.6 mL) injection at varying temperatures (90, 135, 185, and 245 °C) under argon gas darkened the solution. Maintaining the injection temperature for 10 to 12s controlled nanocrystal growth. Rapid cooling with an ice-water bath halted growth, and centrifugation at 5000 rpm for 4 minutes separated Cs_2TiBr_6 nanocrystals from the precipitate. Dissolving the precipitate in 2 ml of hexane enhanced stability and solubility. The colloidal solution was stored in a glovebox to prevent unintended reactions or contamination until later use in experiments or applications [10].

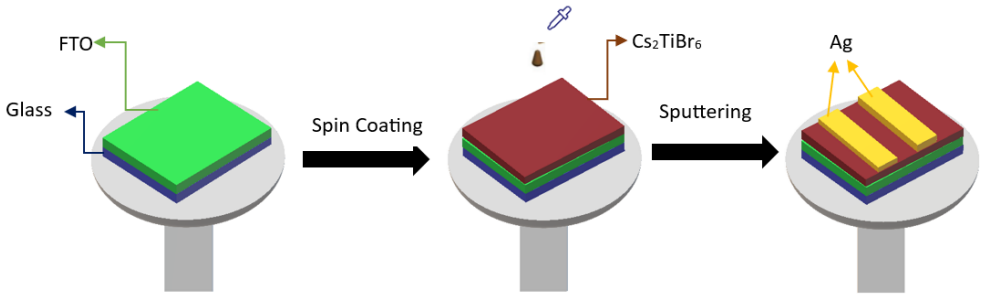

Figure 1. Steps for Fabricating the Proposed PSC.

The complete PSC was fabricated using a straightforward spin coating technique as shown in Fig. 1. Perovskite material was spin-coated onto FTO substrates at 1800 rpm for 30s. Following this, the substrates underwent crucial annealing at 150°C for 10 minutes, enhancing perovskite quality in the PSC. The process concluded with the deposition of a thick layer of silver through sputtering at a rate of 0.3 nm/s. Commonly, traditional device setups employ a TiO_2 layer, often requiring high-temperature calcination to enhance its properties. This approach, though effective, faces issues of thermal stability and defects. In this innovative method, skipping the TiO_2 layer eliminates high-temperature steps,

simplifying fabrication and reducing structural risks due to heat. By deviating from the traditional method of including a compact or mesoscopic TiO_2 layer, this proposed approach provides a new avenue for designing more efficient PSCs.

2.2. Synthesis of Graphene Quantum Dots (GQDs) and modified PSC structure (FTO/GQDs/Cs_2TiBr_6/Ag)

The synthesis of Graphene Quantum Dots (GQDs) involved dispersing 270 mg of Graphene Oxide (GO) in 30 mL of N,N-Dimethylformamide (DMF). Following 30 minutes of ultrasonication, the solution underwent heating at 200 °C in a Teflon-lined autoclave for 8 hours. Subsequently, it was cooled to room temperature, resulting in the formation of a brown, transparent suspension.

For the fabrication of the device, GQDs were spin-coated onto Fluorine-doped Tin Oxide (FTO) at 1400 rpm for 40 seconds, followed by a 75°C, 25-minute thermal treatment prior to perovskite deposition. This strategic enhancement led to the formation of a remarkable FTO/GQDs/Cs2TiBr6/Ag device, which exhibited notable improvements in its photovoltaic parameters as discussed in the next section.

3. Result:

A comprehensive characterization of the intrinsic properties of Cs_2TiBr_6 is performed, as depicted in Figure 2 (a-f). Figure 2 (a) presents the TEM image of Cs_2TiBr_6, showcasing a remarkably dense and uniform surface morphology. XRD analysis of Cs2TiBr6 in Figure 2(b) shows clear 2θ peaks at 29.2°, 31°, 46°, and 56.2°, revealing its crystallographic properties. Figure 2(c) showcases the optical absorbance curves of the Cs_2TiBr_6 absorber on FTO [11]. This data confirms the absorber's efficacy in capturing sunlight with wavelengths shorter than 430 nm. It suggests that the operational spectrum is primarily within the blue light range of the visible light spectrum and there is restricted light material interaction in other light range. In fig. 2 (d), a plot of $(\alpha hv)^2$ versus energy (hv) is presented, allowing for the calculation of the bandgap of Cs_2TiBr_6. The calculated bandgap value is confirmed to be 1.8 eV, falling within the suitable range for the absorber's electronic properties [10].

Figure 2(e) shows the band diagram of the proposed PSCs without ETL & HTL, depicting energy level alignment and electronic transitions governing photovoltaic behavior. The subsequent investigation of the FTO/ Cs_2TiBr_6/Ag device's cross-sectional structure i.e., SEM result is illustrated in fig. 2(f). This examination reveals a vertically oriented architecture, with the Cs_2TiBr_6 layer aligned in a monolayer configuration. This layer possesses a thickness of 290 nm, and it is capped with a thick Ag layer.

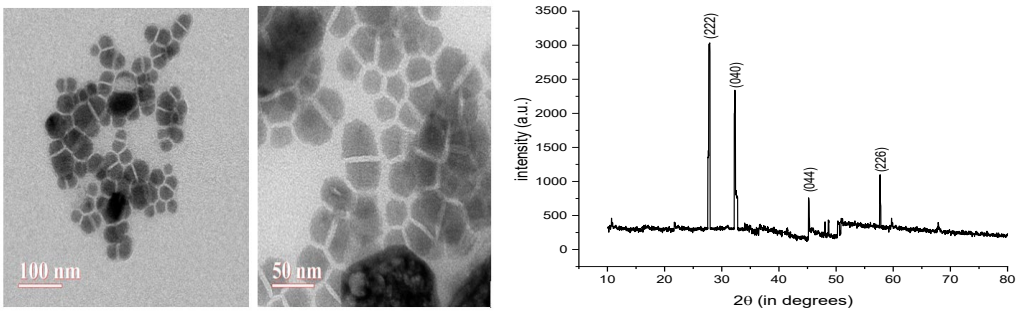

(a) (b)

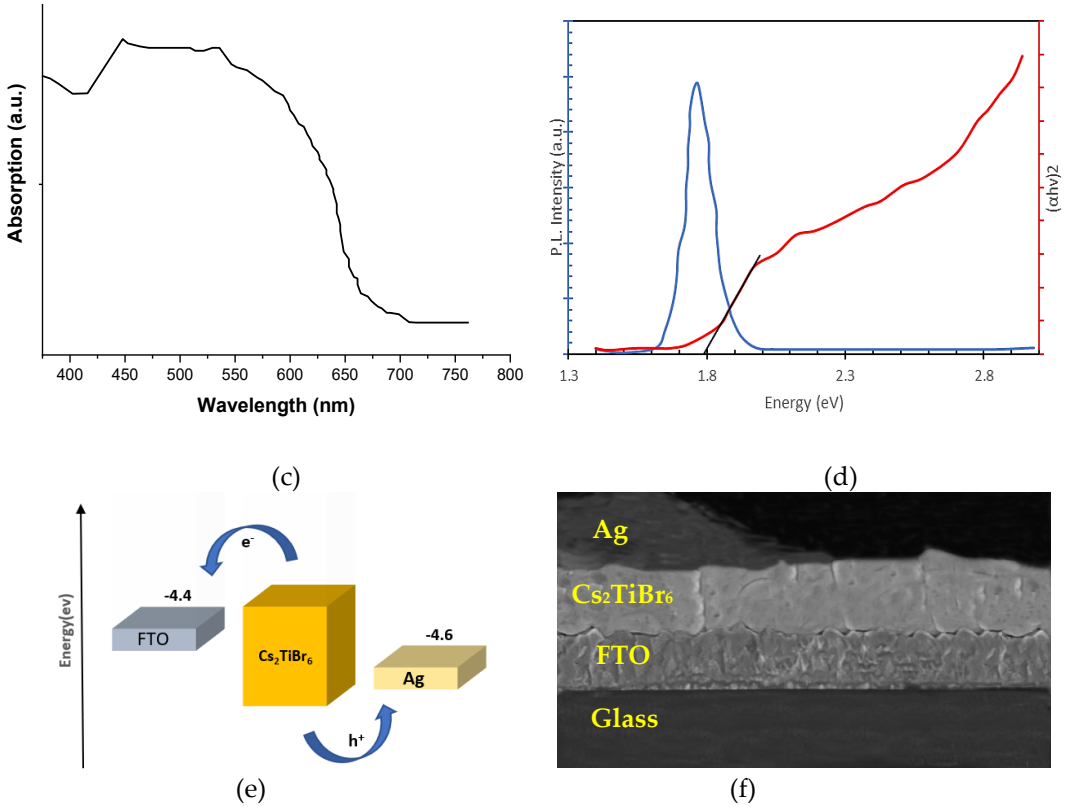

Figure 2. (a) TEM results for synthesized perovskite (b) XRD results for synthesized perovskite (c) UV-Vis results for synthesized perovskite (d) PL sprectrum & Tauc plot of PSC (e) Energy band diagram of PSC (f) SEM result of PSC.

The J-V curve was measured using a Keithley 2400 unit under simulated AM 1.5G sunlight to replicate real solar conditions (light intensity of ≅100mW/cm²). In Fig. 3 (b), the comparative J–V curves of both the proposed PSCs are displayed. The FTO/Cs_2TiBr_6/Ag device achieves a Jsc of 1.78 mA cm^{-2}, Voc of 0.55 V, FF of 44.2% and PCE of 0.89% which can be calculated using eq. (1) and (2). Inefficiency of the present design arises from a significant energy barrier between FTO's work function (-4.4 eV) and Cs_2TiBr_6 's CB (-4.0 eV), causing recombination and poor extraction [12-13]. To counter this, graphene quantum dots (GQDs) were introduced [14-15] and a modified PSC structure (FTO/GQDs/Cs2TiBr6/Ag) is developed as discussed in the previous section. The TEM image of synthesized GQD is shown in fig 3 (a).

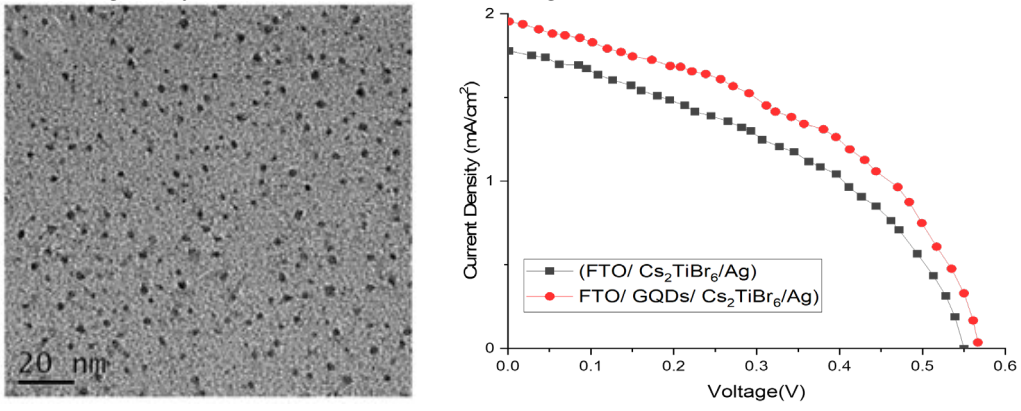

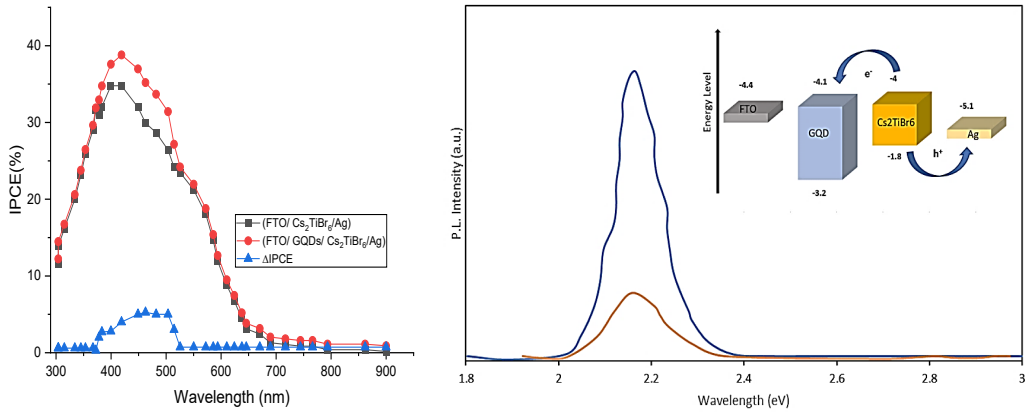

(c) (d)

Figure 3. (a) TEM image of GQD (b) J-V curve (c) IPCE graph (d) PL spectra of Proposed structure.

$$FF = P_{max} / (V_{oc} \times J_{sc}) \quad (1)$$

$$PCE = {(V_{oc} \times J_{sc} \times FF)}/{P_{in}} \quad (2)$$

To confirm enhanced photocurrent, we assessed incident photon-to-current conversion efficiency (IPCE) spectra, shown in fig 3(c). A marked IPCE enhancement appeared from 380 to 550 nm when inserting a GQD layer between perovskite and FTO layers. By integrating GQDs into PSC structure, maximum IPCE rose from 34.6% to 38.79% along with Jsc from 1.78 mA cm^{-2} to 1.95 mA cm^{-2} whereas the fill factor (FF) and open-circuit voltages (Voc) are almost similar. The $\Delta IPCE$ data, which represents internal quantum efficiency spectra, demonstrates a notable improvement, especially around 510 nm, attributed to the inclusion of GQDs. This enhancement is predominantly driven by the absorption of the perovskite's excited state within the GQD layers, in line with the expected minimal absorption by GQD monolayers [16]. As a result, the introduction of GQDs streamlines electron extraction, reduces trapping, and yields an overall efficiency boost that remains consistent across the visible spectrum.

To analyze GQDs' charge extraction behavior, optical characterizations were performed on various Cs_2TiBr_6 films. Emission light intensity correlates with radiative recombination between photogenerated electrons and induced holes. Steady-state photoluminescence (PL) spectrum evaluates charge extraction kinetics. In Figure 3(d), PL spectra of glass/ Cs_2TiBr_6/Ag show a centered peak at 580 nm. The peak intensity deviates in the structure with GQDs. PL peaks lacks due to the weaker light conversion than Cs_2TiBr_6.The significant decrease in photoluminescence results from improved charge extraction facilitated by GQDs. This addition enhances charge transport, thereby mitigating the recombination of photoexcited carriers and lowering photoluminescence emission.

Table 1. Outcomes of the proposed PSC configuration.

Shape	Voc(V)	FF (%)	Jsc (mA cm^{-2})	PCE (%)
FTO/ Cs_2TiBr_6/Ag	0.55	44.2	1.78	0.89
FTO/GQDs/Cs_2TiBr_6/Ag	0.57	45.1	1.95	1.02

The evaluated performance of PSCs both with and without the incorporation of graphene quantum dots (GQDs) are shown in table 1. The structure incorporating GQDs displayed notable improvements: Jsc, Voc, and FF increased to 1.95 mA cm^{-2}, 0.57 V, and 45.1%, leading to PCE of 1.02%. These enhancements can be attributed to enhanced electron extraction, improved charge transport, favorable energy levels, and reduced charge carrier recombination at the interface.

4. Conclusion:

In summary, our study introduces Cs_2TiBr_6 as a promising lead-free perovskite material for solar cells. We utilized a simple spin coating method to fabricate the PSCs, with and without GQDs.These PSCs exhibited notable characteristics, including a high open-circuit voltage Voc of 0.57 V and a commendable FF of 45.10. Although the efficiency was 1.02%, we believe it can be improved by optimizing film thickness, refining surface quality, and enhancing electrical contacts in future iterations.Additionally, the use of Cs_2TiBr_6 as an absorber layer without the need for ETL & HTL positions it as a promising choice for future lead-free perovskite solar cell technology. This approach aligns with our commitment to sustainable and environmentally friendly solar energy solutions.

Author Contributions: Riya Sen was responsible for generating concepts, fabricating, noting result and preparing the initial draft. Menka Yadav provided with valuable suggestion during the work and made corrections in the draft. All the authors have read and agreed to the published version of the manuscript.

Funding: No external Funding is received.

Data Availability Statement: No external data or new data is created.

Conflicts of interest: The authors declare no conflict of interest.

References

1. Jung HS, Park NG. Perovskite solar cells: from materials to devices. Small. 2015 Jan 7;11(1):10-25.
2. Song, Tze-Bin, et al. "Perovskite solar cells: film formation and properties." Journal of Materials Chemistry A 3.17 (2015): 9032-9050.
3. Grätzel M. The light and shade of perovskite solar cells. Nat Mater. 2014 Sep;13(9):838-42.
4. Park, Nam-Gyu. "Perovskite solar cells: an emerging photovoltaic technology." Materials today 18.2 (2015): 65-72.
5. Kim, Jin Young, et al. "High-efficiency perovskite solar cells." Chemical reviews 120.15 (2020): 7867-7918.
6. Bati, Abdulaziz SR, et al. "Next-generation applications for integrated perovskite solar cells." Communications Materials 4.1 (2023): 2.
7. Huang, Y., Liu, T., Liang, C., Xia, J., Li, D., Zhang, H., Amini, A., Xing, G., Cheng, C., Towards Simplifying the Device Structure of High-Performance Perovskite Solar Cells. Adv. Funct. Mater. 2020, 30, 2000863.
8. Duan, J. L., Zhao, Y. Y., He, B. L., Tang, Q. W., Small 2018, 14, 1704443.
9. Yin, Xin, et al. "Novel NiO nanoforest architecture for efficient inverted mesoporous perovskite solar cells." ACS applied materials & interfaces 11.47 (2019): 44308-44314.
10. Grandhi, G.K.; Matuhina, A.; Liu, M.; Annurakshita, S.; Ali-Löytty, H.; Bautista, G., "Lead-free cesium titanium bromide double perovskite nanocrystals." Nanomaterials 11.6 (2021): 1458.
11. Chen, Min, et al. "Cesium titanium (IV) bromide thin films based stable lead-free perovskite solar cells." Joule 2.3 (2018): 558-570.
12. Baena, Juan Pablo Correa, et al. "Highly efficient planar perovskite solar cells through band alignment engineering." Energy & Environmental Science 8.10 (2015): 2928-2934.
13. Dong, Juan, et al. "Controlling the conduction band offset for highly efficient ZnO nanorods based perovskite solar cell." Applied Physics Letters 107.7 (2015).
14. Gan, Xinlei, et al. "Graphite-N doped graphene quantum dots as semiconductor additive in perovskite solar cells." ACS applied materials & interfaces 11.41 (2019): 37796-37803.
15. Acik, Muge, and Seth B. Darling. "Graphene in perovskite solar cells: device design, characterization and implementation." Journal of Materials Chemistry A 4.17 (2016): 6185-6235.
16. Zhu, Zonglong, et al. "Efficiency enhancement of perovskite solar cells through fast electron extraction: the role of graphene quantum dots." Journal of the American Chemical Society 136.10 (2014): 3760-3763.